A New Double Modeling Approach for Dynamic Cardiac PET Studies Using Noise and Spillover Contaminated LV Measurements

Dagan Feng,* *Senior Member, IEEE*, Xianjin Li, and Sung-Cheng Huang, *Senior Member, IEEE*

***Abstract*—A new double modeling approach for dynamic cardiac studies with positron emission tomography (PET) to estimate physiological parameters is proposed. This approach is exemplified by tracer fluorodeoxyglucose (FDG) studies and estimation of myocardial metabolic rate of glucose (MMRGlc). A separate input function model characterising the tracer kinetics in plasma is used to account for the measurement noise and spillover problems of the input curve obtained from the left ventricular region on the PET images. Measured left ventricle (LV) plasma time-activity and tissue time-activity curves are fitted simultaneously with cross contaminations by this input function model and the FDG model. The results indicate that the MMRGlc can be estimated much more accurately and reliably by this new approach. Compared with the traditional method, an improvement of about 20% in the estimated MMRGlc was achieved when the bidirectional spillover fractions are 20% at different noise levels studied. This new double modeling approach using two models fitting both the input and the output functions simultaneously is expected to be generally applicable to a broad range of system modeling.**

I. Introduction

TRACER KINETIC modeling with positron emission tomography (PET) requires measurements of the time-activity curves in both plasma and tissue to estimate physiological parameters. Generally, the plasma time-activity curve (PTAC) and the tissue time-activity curve (TTAC) are used as the input and output functions respectively in the modeling process. In dynamic cardiac PET studies, the input function is often obtained from the left ventricular region on the PET images. Although the use of the measurements directly obtained from left ventricle (LV) images as the PTAC, i.e., the input function, in the modeling process was validated by Weinberg *et al.* [1], there are many factors which can affect the accuracy of these measurements. Amongst others, spillover and the measurement noise are the two major ones which cause the inaccuracy of the input curve thus obtained. In cardiac studies using the tracer fluorodeoxyglucose (FDG) to evaluate the myocardial metabolic rate of glucose (MMRGlc), the radioactivity spillover from the surrounding myocardium to the left ventricle can be very significant, especially at the later part of the study when the concentration in myocardium is much higher than that in the LV. Thus, the simple replacement of PTAC by the direct LV measurements may result in error in MMRGlc estimation.

The spillover problem has been one of the major factors which affect the quantitation of physiological parameters with PET in cardiac studies. Henze *et al.* [2] proposed an analytical method to characterize and solve this problem, and the method was further validated by Herrero *et al.* [3]. However, this analytical solution to the spillover problem is difficult to implement in practice, because it needs the cardiac dimension which is usually not directly available from PET images, and other modalities, such as echocardiography or magnetic resonance imaging (MRI), are often required. Difficulties in the alignment of anatomical planes with different modalities may reduce the accuracy of this approach and additional operational cost limits its application to routine studies. Gamhbir *et al.* [4] proposed a method to incorporate the cardiac dimension as an unknown parameter into the modeling process and estimate it in conjunction with other model parameters. The method, however, used the LV obtained PTAC as an approximation to the true plasma time-activity curve, and the spillover from tissue to blood was not accounted for. Bergmann *et al.* [5] proposed another method in which the spillover (and partial volume) effects were included in the model and estimated together with the blood flow parameter in their study of myocardial blood flow (MBF) with $H_2^{15}O$ and PET. They used the plasma time-activity curves obtained from the left atrial region on the PET images in human studies. Although these curves agreed well with those obtained from femoral artery sampling, the spillover from the surrounding tissue to the left atrial region may not be zero. Iida *et al.* [6] formulated a new model equation in which the recovery coefficients (partial volume effect) in both myocardium and LV and the spillover fractions from blood pool to myocardium (F_{bm}) and from myocardium to blood pool (F_{mb}) were included in the study of MBF with $H_2^{15}O$ and PET. Similarly, Lin *et al.* [7] proposed a new model by reformulating the FDG model and including the bidirectional spillover (F_{bm} and F_{mb}) to study the myocardial glucose utilization rate. However, input measurement noise is not completely removed from their reconstructed discrete input sequence.

Manuscript received September 14, 1994; revised October 10, 1995. This work was supported in part under Grants by ARC and DIATC. *Asterisk indicates corresponding author.*

*D. Feng is with the Basser Department of Computer Science, the University of Sydney, Madsen Building, F09, N.S.W., 2006, Australia (e-mail: feng@cs.su.oz.au).

X. Li is with the Basser Department of Computer Science, the University of Sydney, N.S.W., 2006, Australia.

S. C. Huang is with the Division of Nuclear Medicine and Biophysics, Department of Molecular and Medical Pharmacology and Department of Biomathematics, UCLA School of Medicine, University of California at Los Angeles, Los Angeles, CA 90024-1735 USA.

Publisher Item Identifier S 0018-9294(96)01680-1.

The effect of the input function measurement noise on parameter estimation was studied by Huesman *et al.* [8]. A weighting matrix method for parameter estimation was proposed in order to account for not only the input function noise, but the noise in output measurements as well. His method leads to the reduction of the biases in the estimated parameters. Chen *et al.* [9] later compared different approaches accounting for the input curve measurement noise and found that the use of an input function model to account for the measurement noise could significantly improve the accuracy of parameter estimation.

With the use of PTAC models, the accuracy of parameter estimates can be improved. However, the use of only two-exponential curve and spline curves as PTAC models [9] is not adequate to describe the complex behaviors of the tracer concentration in plasma, as the curves obtained from the actual PET study characteristically contain a period of zero activity at the beginning due to delay from tracer delivery, followed by a rapid rising period, and finally an exponential-like decay period. Feng *et al.* [10] proposed a PTAC model to describe the tracer kinetics in blood vessels. FDG PTAC was represented by a fourth-order exponential curve with a pure delay and a pair of repeated eigenvalues. It has been shown that this seven-parameter PTAC model with a pair of repeated eigenvalues can well describe the tracer behavior in the circulatory system. Detailed simulation studies for using this model to account for the measurement noise and to improve the accuracy of the micro and physiological parameter estimates were reported in [11].

In this study, we develop a model-based method for dynamic cardiac PET FDG studies to account for input curve measurement noise and spillover in the measurement obtained from LV. A seven-parameter input function model describing the kinetics of the radioactive tracer in plasma is adopted, and the two-way spillover fractions (F_{bm} and F_{mb}) are incorporated into the modeling process. Measured LV and tissue time-activity curves are fitted simultaneously by the input function model and FDG model with cross contaminations, and the MMRGlc is then calculated from the fitted micro parameters. Computer simulations were performed to investigate the performance of this approach in accounting for the measurement noise and the spillover in PTAC, and to assess its efficacy in the estimation of MMRGlc. The quantitative results obtained from various simulations indicate that this novel modeling method can effectively overcome the noise and spillover problems in the input curve, and lead to very accurate estimation of MMRGlc. This new modeling approach is expected to be generally applicable to other tracers in dynamic cardiac PET studies and to a broad range of other systems. Moreover, the recovered PTAC is very useful in the generation of parametric images.

II. METHOD

A. The Calculation of the Metabolic Rate of Glucose

The three-compartment FDG model originally proposed by Sokoloff *et al.* [12] and further extended by Phelps *et al.* [13] and Huang *et al.* [14] is used to calculate the myocardial metabolic rate of glucose. The tracer dynamic behavior in tissue is described by the following equation

$$c_t(t) = (B_1 e^{-L_1 t} + B_2 e^{-L_2 t}) \otimes c_p(t) \tag{1}$$

where $c_p(t)$ and $c_t(t)$ denote the true tracer concentrations in plasma and tissue, and B_1, L_1, B_2, and L_2 are macro parameters. From the measurements of both PTAC and TTAC, we can use the above equation to estimate B_1, L_1, B_2, and L_2 via the nonlinear regression technique. The four micro parameters (k_1, k_2, k_3, and k_4) can thus be obtained according to the following relations:

$$k_1 = B_1 + B_2 \quad k_3 = \frac{B_1 L_2 + B_2 L_1}{B_1 + B_2} - \frac{L_1 L_2 (B_1 + B_2)}{B_1 L_1 + B_2 L_2}$$
$$k_2 = \frac{B_1 L_1 + B_2 L_2}{B_1 + B_2} \quad k_4 = \frac{L_1 L_2 (B_1 + B_2)}{B_1 L_1 + B_2 L_2.}$$

The MMRGlc is then calculated using the following formula:

$$\text{MMRGlc} = \frac{1}{LC} \cdot K \cdot C_{glc} \tag{2}$$

where LC is the lumped constant, C_{glc} is the "cold" glucose concentration in plasma, and $K = k_1 k_3/(k_2 + k_3)$.

B. The Plasma Time-Activity Curve

The mathematical expression of the seven-parameter PTAC model proposed by Feng *et al.* [10] is

$$c_p(t) = \begin{cases} [A_1(t-\tau) - A_2 - A_3]e^{\lambda_1(t-\tau)} \\ \quad + A_2 e^{\lambda_2(t-\tau)} + A_3 e^{\lambda_3(t-\tau)} & t > \tau \\ 0 & t \le \tau \end{cases} \tag{3}$$

where $A_1, A_2, A_3, \lambda_1, \lambda_2, \lambda_3$, and τ are parameters with τ representing the time delay of the curve.

C. The New Modeling Approach

Due to the bidirectional spillover between the LV blood pool and myocardium, the noise-free tracer concentrations in LV blood pool $\tilde{c}_p(t)$ and in myocardium tissue $\tilde{c}_t(t)$ obtained from PET images can be described by

$$\tilde{c}_p(t) = c_p(t) + F_{mb} \times c_t(t) \tag{4}$$
$$\tilde{c}_t(t) = c_t(t) + F_{bm} \times c_p(t) \tag{5}$$

where $c_p(t)$ and $c_t(t)$ are the true tracer concentrations in plasma and tissue; F_{mb} and F_{bm} represent the spillover constants from myocardium to blood and from blood to myocardium, respectively. To focus our attention on the correction for the spillover effects and isolate the major problem concerned, we assume that the blood recovery coefficient (F_{bb}) and the tissue recovery coefficient (F_{mm}) to be unity. In Section V, we shall further discuss the reason why we ignore these two parameters. The PET measurements for tracer concentrations in blood $\bar{c}_p(t)$ and in tissue $\bar{c}_t(t)$ are

$$\bar{c}_p(t) = \tilde{c}_p(t) + e_1(t) \tag{6}$$
$$\bar{c}_t(t) = \tilde{c}_t(t) + e_2(t) \tag{7}$$

where $e_1(t)$ and $e_2(t)$ are the PET measurement noise at time t and they are assumed to be additive, independent and Gaussian with zero means. Because the measurements in PET are actually the average values of the total counts during the scanning intervals, the variances of the measurement noise are proportional to the radioactivity concentrations and inversely proportional to the lengths of the scanning intervals [9], [11]. The measurement error variances (Var) can be described by

$$\mathrm{Var}\{e_1(t_i)\} = \frac{c_1 \times \tilde{c}_p(t_i)}{\Delta t_i} \tag{8}$$

$$\mathrm{Var}\{e_2(t_i)\} = \frac{c_2 \times \tilde{c}_t(t_i)}{\Delta t_i} \tag{9}$$

where c_1 and c_2 are the proportional constants, Δt_i is the length of the ith scanning interval, and t_i is the midpoint of Δt_i.

D. Cost Function Used in the Model Fitting

We combine the PTAC model and the TTAC model together and estimate the overall 13 parameters simultaneously by using the weighted nonlinear regression technique. The 13 parameters are coming from three sources: seven are from the analytical definition of PTAC, which determine the shape of the PTAC; four are from the FDG model, which determine the shape of the tissue curve; the remaining two (F_{bm} and F_{mb}) are spillover parameters which determine the spillover fractions between LV and the myocardial tissue. Each parameter makes a different contribution to the model output curves. In addition, one or more venous blood samples $\hat{c}_p(t'_k)$ $(k = 1, 2, \cdots, m)$ taken late in the study are used to improve the numerical identifiability of the spillover fractions. If the total number of sampling points is n, then the cost function for the overall optimization is

$$\begin{aligned}\Phi_1(\theta_1) = &\sum_{i=1}^{n} w_{1i}[\bar{c}_p(t_i) - \tilde{c}_p(t_i)]^2 \\ &+ \sum_{i=1}^{n} w_{2i}[\bar{c}_t(t_i) - \tilde{c}_t(t_i)]^2 \\ &+ \sum_{j=1}^{m} w_{3j}[\hat{c}_p(t'_j) - c_p(t'_j)]^2 \end{aligned} \tag{10}$$

where θ_1 is a parameter vector containing the 13 parameters as mentioned and the weighting factors w_{1i} and w_{2i} are equal to $1/\mathrm{Var}\{e_1(t_i)\}$ and $1/\mathrm{Var}\{e_2(t_i)\}$, respectively, and w_{3j} equals $1/\mathrm{Var}\{$ plasma sample measurement noise at $t'_j\}$. The estimation method which uses $\Phi_1(\theta_1)$ as the cost function is referred to as the *new method.*

For the purpose of comparison, the following objective function for the *traditional method* was also used in parameter estimation using the same data sets

$$\Phi_2(\theta_2) = \sum_{i=1}^{n} w_{2i}\,[\bar{c}_t(t_i) - \check{c}_t(t_i)]^2 \tag{11}$$

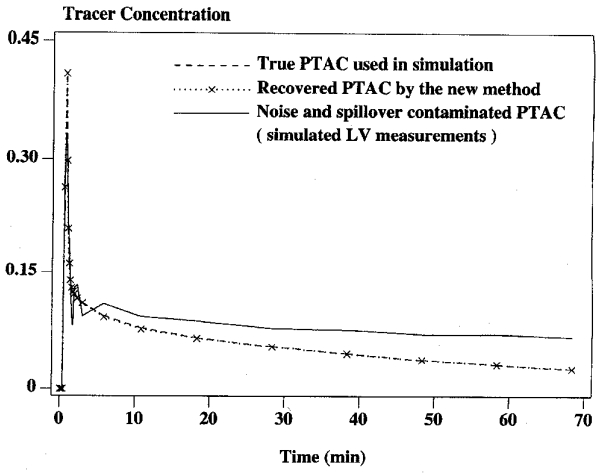

Fig. 1. The dashed line represents the true tracer plasma time-activity curve (which should be the true input function of the FDG model). The solid line represents the noise and spillover contaminated measurement obtained from LV. This curve is generated at a noise level of (6, 5). The spillover from tissue to blood is 20% and the spillover from blood pool to tissue is also 20%. The crosses shown correspond to the recovered input curve values at different sampling time points. These values agree extremly well with their original values on the true tracer plasma time-activity curve.

where the output function $\check{c}_t(t)$ is defined as

$$\check{c}_t(t) = (B_1 e^{-L_1 t} + B_2 e^{-L_2 t}) \otimes \bar{c}_p(t) + F_{bm}\,\bar{c}_p(t) \tag{12}$$

and θ_2 is a parameter vector containing only the five parameters B_1, L_1, B_2, L_2, and F_{bm}. Equation (12) was first used by Hawkins *et al.* [15] to account for the vasculature effect in brain FDG studies and then it was used to account for the blood to tissue spillover in cardiac FDG studies with PET [11], [16], [17]. In (12), $\check{c}_t(t)$ is calculated by directly using the LV-obtained PTAC as the $\bar{c}_p(t)$. Note that the traditional method only accounts for the spillover from the the LV blood pool to myocardium wall but ignores the spillover fraction from the myocardium wall to the LV blood pool.

III. Simulation Studies

Computer simulations were used to assess the performance of the new method under different conditions, i.e., different spillover and noise levels. As in real cases, the spillover and noise levels may vary depending on the size of the region of interest (ROI) drawn on the LV images.

A. Generation of Simulation Data

The true time-activity curve in plasma, $c_p(t)$, is generated from (3) with $A_1 = 5.987, A_2 = 0.0453, A_3 = 0.0881, \lambda_1 = -6.6887, \lambda_2 = -0.2458, \lambda_3 = -0.0181$, and $\tau = 0.537$. These values are obtained from a typical human FDG study. $c_p(t)$ is then used in conjunction with the FDG model (1) to generate the true time-activity curve in tissue $c_t(t)$. The four macro parameters used are $B_1 = 0.0487, L_1 = 0.0009, B_2 = 0.5513$, and $L_2 = 1.85$. They are the average values obtained from a series of human FDG studies [7].

TABLE I
PERCENTAGE ERRORS OF THE ESTIMATED PARAMETER K FROM ITS TRUE VALUE ARE PRESENTED FOR DIFFERENT NOISE LEVEL COMBINATIONS IN PTAC AND TTAC WHEN SPILLOVER F_{mb} EQUALS 17%. RESULTS FROM BOTH THE NEW METHOD, M_{new}, AND THE TRADITIONAL METHOD, M_{old}, ARE GIVEN. LARGER BIASES FROM THE TRADITIONAL METHOD ARE DUE TO THE SPILLOVER FROM TISSUE TO BLOOD FOR WHICH IT DOES NOT ACCOUNT. THE PERCENTAGE ERROR FROM THE NEW METHOD IS LESS THAN 1.5%, SUGGESTING K CAN BE ESTIMATED VERY ACCURATELY. THE SPILLOVER F_{bm} IS FIXED TO 20%

% Errors for estimated K from M_{old} and M_{new}

PTAC noise level	TTAC noise level									
	1		2		3		4		5	
	M_{old}	M_{new}	M_{old}	M_{new}	M_{old}	M_{new}	M_{old}	M_{new}	M_{old}	M_{new}
1	13.2	0.0015	13.7	0.0494	12.9	0.2107	13.9	0.2135	13.0	0.2864
2	13.3	0.2544	13.3	0.1443	13.8	0.1799	13.3	0.6099	13.8	0.1027
3	13.4	0.2135	13.0	0.2301	13.9	0.2851	13.2	0.3688	13.7	0.0246
4	12.8	0.2471	13.0	0.2716	12.9	0.1137	13.8	0.0523	12.9	0.2284
5	13.2	0.3811	13.7	0.2487	14.0	0.3226	14.2	0.5460	14.4	1.1234
6	13.3	0.1135	14.4	0.4019	12.9	0.6284	12.2	0.6808	14.0	0.4089

Both PTAC and TTAC are generated using a sampling schedule which is comparable to that used in a real FDG PET studies [17]. Twenty-two measurements are obtained from 12×10 s scans, 2×40 secs scans, 2×300 s scans, and 6×600 s scans.

The data for $\overline{c}_p(t)$ and $\overline{c}_t(t)$ are generated according to (4)–(7). The noise levels in $\overline{c}_p(t)$ and $\overline{c}_t(t)$ are expressed in terms of their proportional constants c_1 and c_2.

B. The Effect of Noise in Both PTAC and TTAC

To examine the effects of PTAC and TTAC noise at different noise levels, we vary c_1 at 0.00042, 0.0037, 0.01, 0.02, 0.041, and 0.059, corresponding to noise levels ranging from 0.4% to 5% at the last measurement of PTAC. These six noise levels are labeled as level $i(i = 1 - 6)$. The variations of the noise level in PTAC are intended to reflect the varying statistical noise of LV ROI's with different sizes. The values of c_2 used are 0.00508, 0.014, 0.025, 0.035, and 0.046, corresponding to noise levels ranging from 0.7% to 2% at the last measurement of TTAC, as at the end of the study the TTAC is much larger than the PTAC, the noise $e_2(t)$ is expected to be lower than $e_1(t)$. Similar TTAC noise levels have been used in [9], [11] as well. In addition, the TTAC noise levels used here are consistent with those described in [18]. These five noise levels are labelled as level $j(j = 1 - 5)$. Hence, a particular combination of PTAC noise level i and TTAC noise level j is referred to as noise level (i, j).

C. The Effect of Spillover F_{mb} and F_{bm}

One of the objectives in the present study is to assess the performance of the new method to estimate the MMRGlc by taking the spillover factors into consideration. In order to focus on the influence of the spillover fraction from tissue to blood pool F_{mb} on the estimation of K (and other micro parameters in FDG model), we vary the values of F_{mb} at 5%, 8%, 11%, 14%, 17%, and 20% while fixing the spillover from blood to tissue F_{bm} to 20%. For each of the six values of F_{mb}, 100 simulations were performed at each noise level (i, j). For the effect of F_{bm} on the estimation of MMRGlc, we vary the value of F_{bm} from 0% to 35% at a step of 5%. For each of the eight values of F_{bm}, 100 simulations were performed at noise level (1, 5) in PTAC and TTAC while fixing F_{mb} to 20%.

D. Data Analysis

Various statistical criteria, such as estimated parameter mean, bias, sample standard deviation, and coefficient of variation, were calculated from the simulations. For a parameter with true value p, let $\overline{p}$ be the mean of its estimates, SD be the sample standard deviation, and $\Delta p = |p - \overline{p}|$ the bias. The percentage error of the estimated parameter mean $\overline{p}$ from its true value p is $(\Delta p/|p|) \times 100\%$ and the coefficient of variation CV is SD/p.

In this study, the parameter mean $\overline{p}$, the percentage error of the mean, and the coefficient of variation CV are mainly used as criteria to evaluate the performance of the different parameter estimation methods.

IV. RESULTS

A. Construction of the PTAC

Fig. 1 illustrates a typical case in the studies. The dashed line represents the true tracer plasma time-activity curve, i.e., the true input function, used in the simulation. The crosses correspond to the recovered input curve values at different sampling time points. These data were recovered from the contaminated measurements with a noise level of (6, 5) and a tissue to blood pool spillover level of 20%. The solid curve shows one of the typical cases of the noise and spillover contaminated input function with PTAC noise level 6 and a 20% of spillover from tissue to blood pool. It is obvious that the recovered input function from contaminated data agrees very well with the true input curve and the spillover fraction has been successfully removed from the contaminated data. Similar results were obtained for other noise combinations and spillover fractions.

As expected, TTAC noise and the amount of spillover from tissue to blood (F_{mb}) have little influence on the construction of PTAC over the TTAC noise range and spillover fractions used in simulation. In spite of some fluctuations in the estimated PTAC model parameters, the recovered input curves from various spillover fractions and noise levels are quite

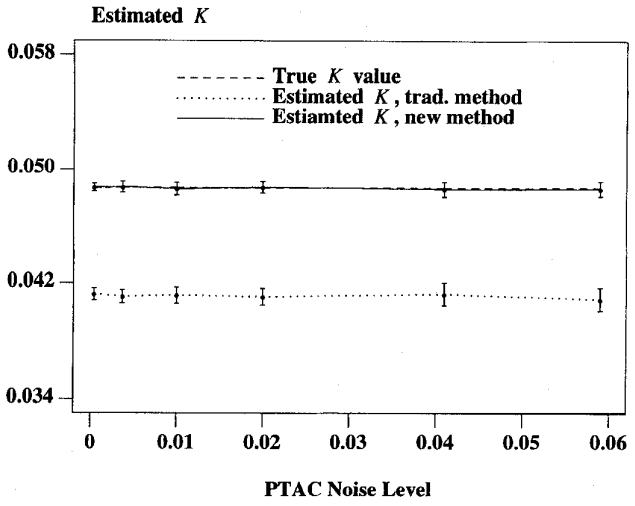

(a)

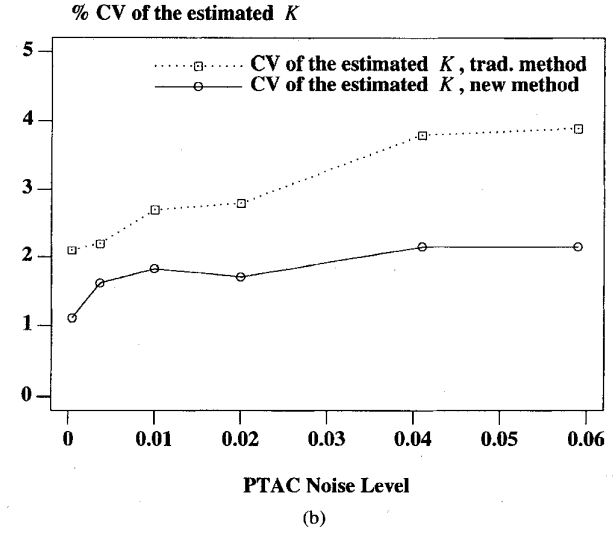

(b)

Fig. 2. (a) Estimation of parameter K from both the traditional method and the new method against PTAC noise. The data presented corresponds to the tissue noise level 1 and a 20% bidirectional spillover fraction between tissue and blood pool. The underestimation of K by the traditional method is mainly due to the spillover from tissue to blood. The error bars represent the SD of the estimated K at different PTAC noise levels. (b) Coefficient of variation (CV) of the estimated K against PTAC noise. The CV's of the estimated K from both the traditional method and the new method increase as PTAC noise increases. However, the increasing rate of the CV from the traditional method is higher than that from the new method. Its CV value is almost twice as big as that from the new method at the highest noise level, suggesting that K can be estimated more reliably by the new method.

consistent with the true input function in terms of their shapes and the areas covered.

B. Estimation of K

1) The Effects of Noise in PTAC and TTAC: The effect of noise in PTAC and TTAC on the estimated K by the new method is not significant, although the noise does contribute some uncertainties to the estimate of K. The percentage errors in the estimated parameter K from its true value at different

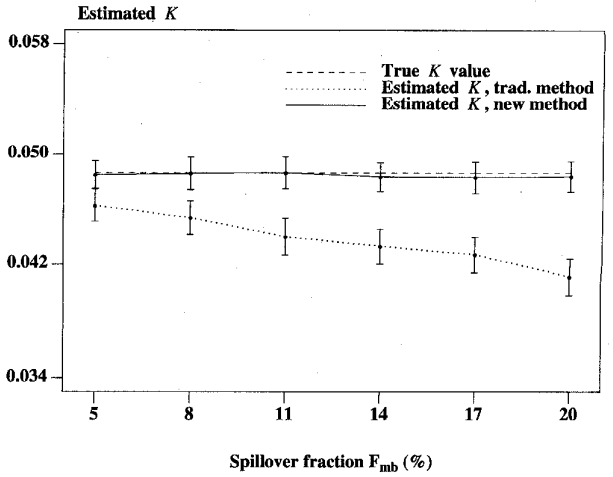

Fig. 3. Estimated parameter K as a function of spillover F_{mb}. The data was obtained at a noise level of (6, 4) in PTAC and TTAC and a fixed 20% spillover F_{bm}. Estimates of K from the traditional method under the same noise and spillover conditions are also plotted for comparison. Note that the more the spillover, the more the underestimation of K by the traditional method. In contrast, by taking the spillover F_{mb} into consideration, the new method can estimate K very accurately (the bias is less than 1.5% of its true value). The error bars represent the SD of the estimated K at different spillover fractions.

noise level combinations in PTAC and TTAC are presented in Table I. Fig. 2(a) shows the estimate of K as a function of PTAC noise level when spillover F_{mb} equals 20%. It is clear that the new method can provide an unbiased estimation of K, while the traditional method, which does not account for the spillover from tissue to blood, underestimates K by about 16%. Noise in PTAC tends to increase the SD of the estimated K by the two methods. However, the magnitude of this increase from the new method is smaller than that from the traditional method. Fig. 2(b) plots the corresponding CV's of the data in Fig. 2(a). As is shown, the new method significantly reduces the CV of the estimated K. In addition, the increasing rate of CV as a function of PTAC noise from the new method is smaller than that of the traditional method. For every combination of PTAC noise and TTAC noise in the simulations, the CV of the estimated K was less than 6%, suggesting that K can be estimated very reliably by the new method.

2) The Effects of Spillover F_{mb} and F_{bm}: Fig. 3 shows the estimate of K as a function of spillover from tissue to blood (F_{mb}). The data was obtained at noise level (6, 4) in PTAC and TTAC. Notice that parameter K is considerably underestimated by the traditional method which does not account for the spillover from tissue to blood. The more the spillover, the more the underestimation of K. In contrast, different spillover of radioactivity from tissue to blood has little effect on the estimated K by the new method. The slight underestimation of K at higher spillover fractions in the figure is due to the effect of noise in PTAC and TTAC. For every spillover fraction simulated, the bias of the estimated K was less than 1.5% by the new method.

The effect of spillover from blood to tissue (F_{bm}) on the estimated K was also studied. Fig. 4(a) illustrates the

simulation results obtained at noise level (1, 5) in PTAC and TTAC with the spillover F_{mb} fixed to 20%. Results from both the new method and the traditional method are plotted. The underestimation of K by the traditional method is mainly due to the spillover from tissue to blood (see the estimated K at $F_{bm} = 0$). That is, by only taking the spillover from blood pool to tissue into consideration, the traditional method can lead to considerable underestimation of K. In addition, it is unable to completely get rid of the effect of spillover from blood to tissue when a fraction of spillover from tissue to blood exists. This can be seen from the descending dotted line in the figure. The new method, on the other hand, can estimate K quite accurately as shown. In addition, the CV of the estimated K from the new method is greatly improved as compared to that from the traditional method as illustrated in Fig. 4(b).

C. Estimation of F_{mb}, F_{bm}, and k_4

Table II gives the estimates of F_{mb} and F_{bm} with respect to the spillover values used in the simulation. Results from both the new method and the traditional method at a particular noise level in PTAC and TTAC are presented. While the traditional method provides no estimation of F_{mb}, the new method can recover the F_{mb} values very accurately. The estimates of F_{bm} are available from both methods. Although not significantly different, the estimated F_{bm} obtained with the new method are slightly larger, therefore slightly closer to its true value, than those obtained with the traditional method.

The calculation of K does not explicitly require the value of k_4. However, the value of k_4 can influence the values of the other rate constants k_1, k_2, and k_3 when the rate constants are estimated [14]. It has been observed [7] that the value of k_4 can be overestimated by the traditional method. Therefore, the estimation of k_4 is one of our main concerns in the present study. The estimates of k_4 from both methods at a particular noise level are shown in Fig. 5 as a function of spillover F_{mb}. It is seen that the new approach proposed can provide much more accurate estimates of k_4 when compared with the traditional method, which tends to overestimate k_4.

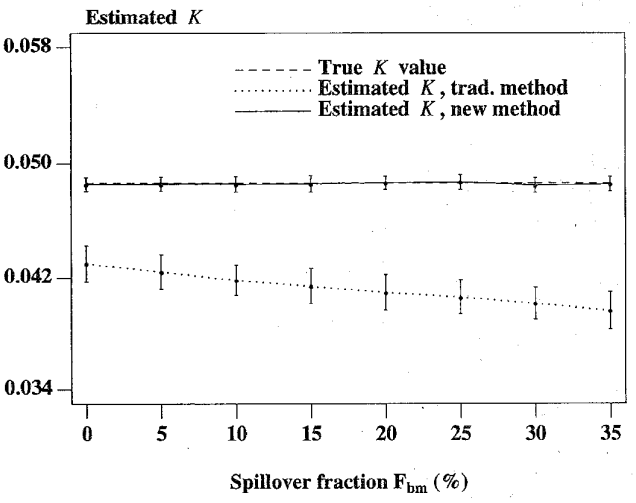

(a)

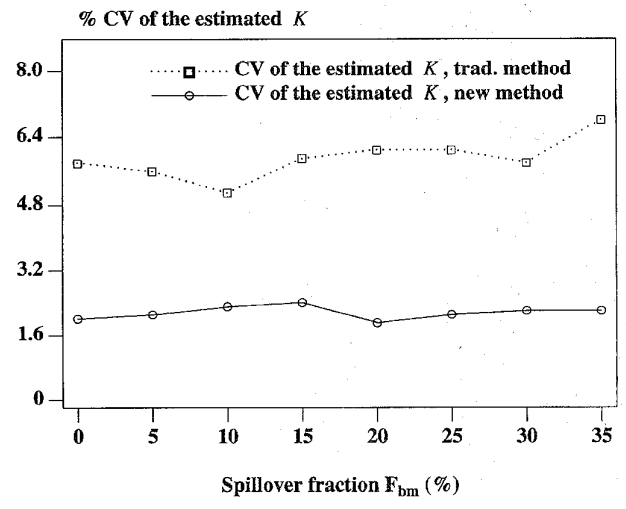

(b)

Fig. 4. (a) Estimated parameter K as a function of spillover F_{bm}. The data was obtained at noise level (1, 5) in PTAC and TTAC with a 20% spillover F_{mb}. This figure illustrates that the spillover from tissue to blood can cause a significant underestimation of K even though the spillover from blood to tissue has been taken into account in the traditional modeling approach. When the spillover coefficient increases, the bias in the estimated K increases. On the other hand, the new modeling approach which takes the spillover in both dirctions into account can achieve unbiased estimation of K, as shown by the solid line in the figure. The error bars represent the SD of the estimated K at different spillover fractions. (b) Coefficient of variation (CV) of the estimated K as a function of spillover F_{bm}. In the diagram, the CV's from the traditional method are about two times greater than those obtained from the new method. In other words, K can be estimated much more accurately and reliablely by using the new method.

V. Discussion

In dynamic cardiac FDG studies with PET to quantify the regional myocardial glucose utilization, PTAC is usually obtained by drawing ROI's positioned on LV PET images. However, LV PTAC is contaminated by the spillover of radioactivity in the surrounding myocardium and can cause considerable error in the estimated MMRGlc (Fig. 2). Measurement noise due to counting statistics is another error source which causes the inaccuracy of PTAC and further affects the MMRGlc estimation. In the present study, a model-based method has been proposed in order to overcome these problems, i.e., spillover and PTAC measurement noise. Computer simulations were conducted to demonstrate the feasibility of this method in tackling these problems.

A seven-parameter PTAC model was adopted. The purpose of using this tracer plasma model is twofold. Firstly, by means of describing the input function via a model, it not only allows the spillover factors of the bidirectional contaminations between myocardium and LV blood pool to be included in the modeling procedure, but also facilitates the separation of spillover factors in the fitting procedure. Secondly, using this plasma model can filter out the measurement noise.

In our study, we had no difficulty in fitting the seven-parameter PTAC model, as each of these seven parameters is associated with a different segment of the curve [10].

TABLE II

ESTIMATED F_{mb} AND F_{bm} BY BOTH THE NEW METHOD, M_{new}, AND THE TRADITIONAL METHOD, M_{old}. THE DATA IN THE TABLE CORRESPOND TO THE NOISE LEVEL (6, 5) IN PTAC AND TTAC AND SPILLOVER F_{bm} OF 20%. THE ESTIMATED F_{mb} IS NOT AVAILABLE FROM THE TRADITIONAL METHOD. NOTE THAT F_{mb} CAN BE RECOVERED VERY ACCURATELY FROM THE NEW METHOD, AND THE ESTIMATES OF F_{bm} FROM THE NEW METHOD ARE SLIGHTLY CLOSER TO ITS TRUE VALUE (0.20)

	Estimated spillover constants from M_{old} and M_{new}			
	Estimated F_{mb}		Estimated F_{bm}	
F_{mb}	M_{old}	M_{new}	M_{old}	M_{new}
0.05	—	0.0492 ± 0.0051	0.1730 ± 0.0991	0.1834 ± 0.0786
0.08	—	0.0796 ± 0.0058	0.1804 ± 0.0683	0.1846 ± 0.0783
0.11	—	0.1085 ± 0.0057	0.1618 ± 0.0754	0.1795 ± 0.0815
0.14	—	0.1395 ± 0.0060	0.1710 ± 0.0582	0.1761 ± 0.0835
0.17	—	0.1700 ± 0.0063	0.1839 ± 0.0766	0.1871 ± 0.0708
0.20	—	0.1999 ± 0.0069	0.1742 ± 0.1028	0.1894 ± 0.07880

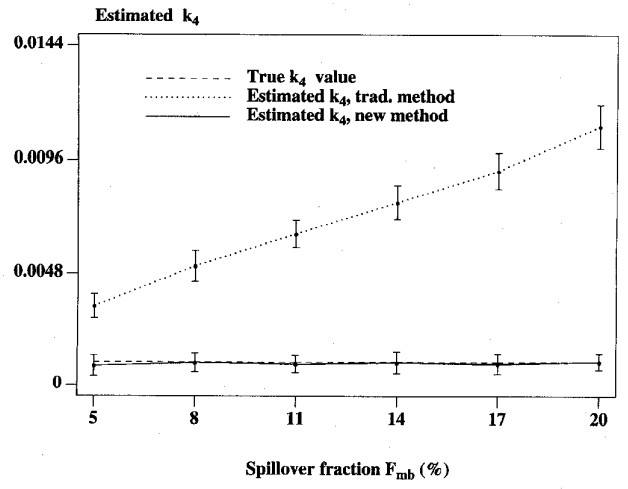

Fig. 5. Estimated k_4 as a function of spillover F_{mb}. The data presented corresponds to a noise level of (6, 2) in PTAC and TTAC with a 20% spillover F_{bm}. Note that the traditional method overestimates k_4 considerably due to the spillover from tissue to blood. The more the spillover F_{mb}, the more the overestimation of k_4. The simulation results summarized in this figure demonstrate that the new method can estimate k_4 very accurately and reliably. The error bars represent the SD of the estimated k_4 at different spillover fractions.

Particularly, parameters $\lambda_1, \lambda_3, A_3$, and τ can be estimated very reliably. Although A_1, A_2, and λ_2 are more sensitive to the measurement noise, the shape of the overall curve constructed has very little change at different measurement noise levels. Therefore, the estimation of the physiological parameter MMRGlc is very stable.

Errors in parameter k_4 can have a big influence on the estimation of K. Based on the simulation study, overestimation of k_4 leads to the underestimation of K. This is consistent with the results reported and discussed in [17]. Since k_4 can be estimated very accurately with the proposed method, those part of errors in the estimated K, which is from the inaccurate estimate of k_4, can be effectively eliminated.

The simulation study has demonstrated that the new method is effective in overcoming the measurement noise and spillover problems, and it is able to provide an accurate and reliable estimate of MMRGlc. The estimated K values are within 98.5% of its true value under all the noise levels and spillover conditions simulated. The two spillover factors F_{bm} and F_{mb} can also be recovered with reasonable accuracy.

In the model fitting procedure, several measurements from real venous blood samples may be needed in order to improve the numerical identifiability of the spillover parameters. The results presented in the previous section were obtained when the true PTAC values at the last two points were used (i.e., $m = 2$ in the cost function $\Phi_1(\theta_1)$) and their weights were chosen to be 20 times larger than that of the last point of $\tilde{c}_p(t)$, as we assumed that the variance of PET measured $\tilde{c}_p$ was equal to $\tilde{c}_p$ and the variance of c_p measured from blood samples was about 5% of its mean. The fitting procedure usually converged within 30 iterations. As the tracer plasma concentration can be measured far more accurately from direct plasma samples than by an external scanner, especially when the tracer plasma concentration is very weak at the end of the study, we carried out a simulation with only one blood sample (i.e., $m = 1$) with $w_{31} = 100 \times w_{1n}$ and we also obtained very similar results and the same conclusion as discussed above. In general, two to three measurements at later time may be preferable in practical applications.

The use of the new modeling method can successfully account for the bidirectional spillover between LV and myocardial wall and remove the measurement noise in the LV-obtained PTAC to achieve the noninvasive measurement of MMRGlc. As in cardiac studies in [7], [16], and [17] to estimate the MMRGlc, we did not address the partial volume effects either in the current study so as to focus our attention on the major subject concerned. If the dynamic data are obtained from the reconstructed images, neglecting the two recovery coefficients can cause errors in the estimated parameters [5], [19]–[21]. The blood recovery coefficient (F_{bb}) and the tissue recovery coefficient (F_{mm}) can be incorporated into (4) and (5). However, additional information in regard to the partial volume effects is required to provide enough constraint on these two new parameters to achieve a good identifiability. This complicated situation is under investigation and results will be reported once they are available.

According to the simulation results, the method proposed is promising for use in dynamic cardiac FDG studies to provide noninvasive quantitation of MMRGlc. The application to human studies is currently underway, and the results will be reported separately.

In conclusion, the proposed modeling approach, which takes the bidirectional spillover into account, is effective in overcoming the spillover problem in cardiac studies with PET

without the need for extra knowledge such as the cardiac dimensions. It provides a possible way to directly use the LV measurements or other spillover contaminated measurements as the input function in the tracer kinetic modeling process to estimate physiological parameters noninvasively. Second, it allows larger ROI's to be drawn over the LV in dynamic PET images to increase the signal-noise ratio and to improve the accuracy of the LV measurements. Third, it can construct a PTAC from the noise and spillover contaminated LV measurements, and thus provide a spillover corrected and noise filtered PTAC, which can further be used to estimate MMRGlc for other ROI's and to generate MMRGlc parametric images. Finally, it can provide a very accurate and reliable estimation of MMRGlc, a physiological parameter which has been shown to be useful for defining tissue viability in patients with ischemic heart disease [22]. This new double modeling approach is expected to be generally applicable to other tracers in dynamic cardiac PET studies and to a broad range of other systems.

ACKNOWLEDGMENT

The authors are grateful to B. Hutton, S. Meikle, R. Fulton, D. Bailey, and B. A. Ardekani from the Department of Nuclear Medicine, Royal Prince Alfred Hospital, Australia, for their helpful criticisms and comments on this work.

REFERENCES

[1] I. N. Weinberg, S. C. Huang, E. J. Hoffman, L. Araujo, C. Nienaber, M. GroverMckey, M. Dahlbom, and H. Schelbert, "Validation of PET-acquired input functions for cardiac studies," *J. Nucl. Med.*, vol. 29, no. 2, pp. 241–247, 1988.

[2] E. Henze, S. C. Huang, O. Ratib, E. Hoffman, M. E. Phelps, and H. R. Schelbert, "Measurements of regional tissue and blood-pool radiotracer concentrations from serial tomographic images of the heart," *J. Nucl. Med.*, vol. 24, no. 11, pp. 987–996, 1983.

[3] P. Herrero, J. Markham, D. W. Myears, C. J. Weinheimer, and S. R. Bergmann, "Measurement of myocardial blood flow with positron emission tomography: Correction for count spillover and partial volume effects," *Math. Comput. Modeling*, vol. 11, pp. 807–812, 1988.

[4] S. S. Gambhir, "Quantitation of the physical factors affecting the tracer kinetic modeling of cardiac positron emission tomography data," Ph.D. thesis, Univ. California, Los Angeles, 1990.

[5] S. R. Bergmann, P. Herrero, J. Markham, C. J. Weinheimer, and M. N. Walsh, "Noninvasive quantitation of myocardial blood flow in human subjects with oxygen-15-labeled water and positron emission tomography," *J. Am. College Cardiol.*, vol. 14, no. 3, pp. 639–652, 1989.

[6] H. Iida, C. G. Rhodes, R. Silva, L. I. Araujo, P. M. Bloomfield, A. A. Lammertsma, and T. Jones, "Use of the left ventricular time-activity curve as a noninvasive input function in dynamic oxygen-15-water positron emission tomography," *J. Nucl. Med.*, vol. 33, no. 9, pp. 1669–1677, 1992.

[7] K. P. Lin, S. C. Huang, Y. Choi, R. Brunken, H. Schelbert, and M. Phelps, "A method for correcting myocardium to blood pool spillover in dynamic cardiac PET FDG studies," *J. Nucl. Med.*, vol. 33, no. 5, pp. 882, 1992.

[8] R. H. Huesman and B. M. Mazoyer, "Kinetic data analysis with a noisy input function," *Phys. Med. Biol.*, vol. 32, no. 12, pp. 1569–1579, 1987.

[9] K. Chen, S. C. Huang, and D. C. Yu, "The effects of measurement errors in the plasma radioactivity curve on parameter estimation in positron emission tomography," *Phys. Med. Biol.*, vol. 36, no. 9, pp. 1183–1200, 1991.

[10] D. Feng, S. C. Huang, and X. Wang, "Models for computer simulation studies of input functions for tracer kinetic modeling with positron emission tomography," *Int. J. Bio-Med. Comput.*, vol. 32, pp. 95–110, 1993.

[11] D. Feng and X. Wang, "A computer simulation study on the effects of input function measurement noise in tracer kinetic modeling with positron emission tomography (PET)," *Comput. Biol. Med.*, vol. 23, no. 1, pp. 57–68, 1993.

[12] L. Sokoloff, M. Reivich, C. Kennedy, M. H. D. Rosiers, C. S. Patlak, K. D. Pettigrew, O. Sakurada, and M. Shinohara, "The [^{14}C]deoxyglucose method for the measurement of local cerebral glucose utilization: Theory, procedure, and normal values in the conscious and anesthetized albino rat," *J. Neurochem.*, vol. 28, pp. 897–916, 1977.

[13] M. E. Phelps, S. C. Huang, E. J. Hoffman, C. J. Selin, L. Sokoloff, and D. E. Kuhl, "Tomographic measurement of local cerebral glucose metabolic rate in humans with (F-18)2-fluoro-2-deoxy-D-glucose: Validation of method," *Ann. Neurol.*, vol. 6, pp. 371–388, 1979.

[14] S. C. Huang, M. E. Phelps, E. J. Hoffman, K. Sideris, C. J. Selin, and D. E. Kuhl, "Noninvasive determination of local cerebral metabolic rate of glucose in man," *Am. J. Physiol.*, vol. 238, pp. E69–E82, 1980.

[15] R. A. Hawkins, M. E. Phelps, and S. C. Huang, "Effects of temporal sampling, glucose metabolic rates, and disruptions of the blood-brain barrier on the FDG model with and without a vascular compartment: Studies in human brain tumours with PET," *J. Cerebral Blood Flow Metabol.*, vol. 6, pp. 170–183, 1986.

[16] S. S. Gambhir, M. Schwaiger, S. C. Huang, J. Krivokapich, H. R. Schelbert, C. A. Nienaber, and M. E. Phelps, "Simple noninvasive quantification method for measuring myocardial glucose utilization in humans employing positron emission tomography and fluorine-18 deoxyglucose," *J. Nucl. Med.*, vol. 30, no. 3, pp. 359–366, 1989.

[17] Y. Choi, R. A. Hawkins, S. C. Huang, S. S. Gambhir, R. C. Brunken, M. E. Phelps, and H. R. Schelbert, "Parametric images of myocardial metabolic rate of glucose generated from dynamic cardiac PET and 2-[^{18}F]fluoro-2- deoxy-D-glucose studies," *J. Nucl. Med.*, vol. 32, pp. 733–738, 1991.

[18] S. Jovkar, A. C Evans, M. Diksic, H. Nakai, and Y. L. Yamamoto, "Minimisation of parameter estimation errors in dynamic PET: Choice of scanning schedules," *Phys. Med. Biol.*, vol. 34, no. 7, pp. 895–908, 1989.

[19] E. J. Hoffman, S. C. Huang, and M. E. Phelps, "Quantitation in positron emission computed tomography—1: Effect of object size," *J. Comput. Assist. Tomog.*, vol. 3, no. 6, pp. 299–308, June 1979.

[20] G. Wisenberg, H. R. Schelbert, E. J. Hoffman, M. E. Phelps, G. D. Robinson, C. E. Selin, J. Child, D. Skorton, and D. E. Kuhl, "*In vivo* quantitation of regional myocardial blood flow by positron emission tomography," *Circ.*, vol. 6, pp. 1245, 1258 1981.

[21] H. Iida, I. Kanno, A. Takahashi, S. Miura, M. Murakami, K. Takahashi, Y. Ono, F. Shishido, A. Inugami, N. Tomura, S. Higano, H. Fujita, H. Sasaki, H. Nakamichi, S. Mizusawa, Y. Kondo, and K. Uemura, "Measurement of absolute myocardial blood flow with $H_2^{15}O$ and dynamic positron-emission tomography," *Circ.*, vol. 78, no. 1, pp. 104–115, 1988.

[22] R. C. Marshall, J. H. Tillisch, M. E. Phelps, S. C. Huang, R. Carson, E. Henze, and H. R. Schelbert, "Identification and differentiation of resting myocardial ischemia and infarction in man with positron computed tomography, ^{18}F-labeled fluorodeoxyglucose and N-13 ammonia," *Circ.*, vol. 67, no. 4, pp. 766–778, 1983.

Dr. Dagan Feng (S'88–M'88–SM'94) received the M.E. degree in electrical engineering from Shanghai Jiao Tong University in 1982, M.Sc. degree in biocybernetics and Ph.D. degree in computer science from the University of California, Los Angeles, in 1985 and 1988, respectively.

Since 1988 he has worked as an Assistant Professor at the University of California, Riverside, a Lecturer and then a Senior Lecturer at the University of Sydney. His main research interests are modeling, simulation, function imaging and signal processing with biomedical applications.

Dr. Feng received the Crump Prize for Excellence in Medical Engineering in 1987.

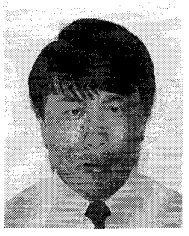

Xianjin Li was born in Shanxi, China, in 1963. He received the B.S. degree in computer science from Nankai University, Tianjin, China, in 1983 and the M.E. degree in computer science and engineering from Xian Jiaotong University, Xian, in 1986. Since 1992, he has been a Ph.D student in the Basser Department of Computer Science, the University of Sydney, working on computer methodology with biomedical applications.

He joined the Department of Computer and System Science of Nankai University in 1986 as a Member of Academic Staff. His research interests include computer modeling, image processing and analysis with biomedical applications.

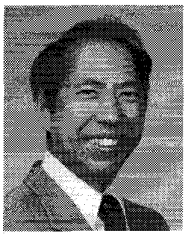

Sung-Cheng Huang (S'68–M'74–SM'91) received the BS degree in electrical engineering from National Taiwan University in 1966, and the Ph.D. degree from Washington University, St. Louis, in 1973.

He was involved in the development and design of early X-ray (CT scanners) from 1974–1977 at Picker Corp., and has been with UCLA since 1977. Currently, he is Professor in department of Molecular and Medical Pharmacology and department of Biomathematics. He is Associate Director of the Crump Institute for Biological Imaging in UCLA School of Medicine, and is Deputy Chief Editor of Journal of Cerebral Blood Flow and Metabolism. His primary research interest is on tracer kinetic modeling that uses mathematical and engineering methods to relate physical measurements of tracer dynamics to biomedical information. He also works on tomographic image reconstruction and biomedical image analysis and registration.